Wu and Song
Journal of Engineering and Applied Science (2024) 71:152
https://doi.org/10.1186/s44147-024-00483-x

Journal of Engineering and Applied Science

RESEARCH Open Access

Three-dimensional artistic design method of ceramic products based on recurrent neural network technology

Xueting Wu[1] and Jungyu Song[2*]

*Correspondence:
sjk1515562@163.com

[1]College of Ceramics, Wuxi Vocational Institute of Arts & Technology, Wuxi 214200, Jiangsu, China
[2] Sangmyung University, Cheonan 31006, South Korea

Abstract

Three-dimensional digital technology has made breakthroughs and shown unique advantages in all walks of life. On the basis of practicality, the three-dimensional artistic design of ceramic products gradually adds some aesthetic, artistic design elements, which brings beautiful enjoyment to people's lives and makes people's lives colorful. This paper presents a three-dimensional artistic design method for ceramic products based on RNN (recurrent neural network) technology. With the establishment of the 3D YOLOv3 framework, the new model training is faster and more stable, the convergence speed of the loss function is faster, and the reconstructed 3D model is more accurate. After training for a certain number of times, the network gradually becomes stable, the accuracy rate is kept at 95%, and the loss function value is reduced below 0.2. The accuracy of the network model and the precision of semantic segmentation are improved. The semantic segmentation and object recognition under 3D scene reconstruction studied in this paper have certain theoretical value and high feasibility.

Keywords: RNN, Ceramic products, Three-dimensional artistic design

Introduction

The renewal of ceramics has made people's lives colorful, fashionable, and with a high degree of visual beauty, showing people's lives a unique charm of China. In the process of making ceramics, the requirements and standards of detail design in related modeling are also increasing. By adding relevant details to the overall design, it can not only enhance the aesthetic feeling and aesthetics of the whole ceramic works but also make the related works more vivid. In addition, it can effectively enhance the artistic effect of the whole ceramic work. With the improvement of modern people's living standards, the development of ceramic jewelry in China is rapidly rising. These years, it has developed rapidly, showing the characteristics of localization. People are gradually turning their attention from traditional expensive jewelry materials to new popular materials. For jewelry manufacturers and designers, how to meet this demand of consumers has become a new mission.

Ceramic jewelry characterized by hand-made has not only the characteristics of ceramic culture but also the characteristics of handicraft and folk art. Jiang et al. mentioned that computer-aided pattern creation and design can make up for the defects of

hand-made, which is conducive to modification at any time. At the same time, unexpected effects often appear in the creation [1]. Neusser et al. scanned a single ceramic product accordingly. Then they classified the tree species according to the extracted characteristic parameters [2]. The design and production of ceramic products are undergoing unprecedented changes [3]. As an ancient and exquisite art, ceramic design not only carries profound cultural heritage but also faces the important task of combining with modern technology to create more innovative and personalized products [4]. In this context, the 3D art design method for ceramic products based on recursive neural network technology has emerged, bringing new development opportunities to the field of ceramic design. Traditional ceramic product design mainly relies on the personal experience and artistic cultivation of designers, completed through hand drawing or computer-aided design software. However, this method has limitations in terms of efficiency, innovation, and personalization [5]. With the continuous progress of computer vision and deep learning technology, people are beginning to explore the application, in order to achieve more efficient and intelligent design processes [6].

Recurrent neural networks (RNNs), as an important model in the field of deep learning, have the ability to process sequential data and are particularly suitable for processing time-dependent data. In ceramic product design, designers usually need to consider the correlation and mutual influence between multiple design elements, such as shape, color, and texture. These design elements can be viewed as a type of sequential data, learned and predicted through RNN models, to generate innovative and personalized design solutions [7]. The 3D art design method for ceramic products based on recursive neural network technology aims to learn and understand the design rules of ceramic products through training RNN models and generate 3D art design works that meet the requirements of designers. This method can automatically extract the associations and mutual influences between design elements and intelligently recommend and optimize them based on the designer's input [8]. Through this approach, designers can improve design efficiency and personalization while maintaining artistic and creative qualities, better meeting market demand and consumer expectations. Compared with the previous rule-based and feature-based relationship extraction methods, the method based on the machine learning model reduces manual operation.

Since the appearance of ceramics, the relevant producers have been constantly designing and researching the shapes of ceramics in the process of making ceramics, thus creating various ceramic works. The introduction of three-dimensional digital technology into the design of traditional arts and crafts products can attract students' attention and stimulate people's love for traditional arts and crafts products with the help of modern science and technology. It can be said that three-dimensional digital technology is a communication bridge to promote cultural inheritance and dissemination. This topic aims to apply the generated three-dimensional semantic concept to practice based on RNN (recurrent neural network) technology. On the basis of traditional three-dimensional artistic design of ceramic products, it can influence the content and form of three-dimensional artistic design of ceramic products, improve ceramic production efficiency, achieve a convenient and accurate effect, save the cost of three-dimensional artistic design of ceramic products, and also bring new vitality. In addition, this method has practical value for similar occasions, such as the reconstruction of cultural relics and the design of other handicrafts.

This article proposes a three-dimensional artistic design method for ceramic products based on recursive neural network (RNN) technology. Using the 3D YOLOv3 framework, this framework has been optimized and improved on the basis of YOLOv3, making model training faster and more stable. The 3D YOLOv3 framework improves the convergence speed of the loss function, thereby enhancing the accuracy of the reconstructed 3D model. This study has certain theoretical value in semantic segmentation and object recognition under three-dimensional scene reconstruction. The proposed 3D art design method for ceramic products based on RNN technology has high feasibility and is expected to be widely applied in practical applications, bringing people more diverse and colorful artistic enjoyment.

Methods

RNN technology overview

As a computational model of information processing [9, 10], It is unclear to what extent the artificial neural network fits the function of the brain. Neural networks can automatically learn valuable experiences from complex and seemingly unrelated information. They can be used in predictive modeling, adaptive control, optimal combination, and other fields that can be trained and learned according to data sets.

Rn is a kind of DNN (deep neural network) adapted to the sequence data. Unlike feedforward neural networks, which accept data with a specific structure as input, RNNs transmit the network state in an internal loop. Although GPU is still the first choice for training neural networks at present, it is not easy to popularize the inference-based scene, such as edge computing, because of its cost and power consumption. RNN has been successful in a variety of application scenarios related to sequence processing, including speech recognition, machine translation, and scene analysis, and various variants have been derived continuously.

In the traditional neural network model, each layer is connected with each other, while the nodes between each layer are unconnected [11]. Therefore, the neural network with this structure can deal with limited problems and cannot deal with time-series data. In RNN, the current. Because of the special structure of sequential memory, RNN is often used in natural language processing tasks. The RN model and its expanded model structure are shown in Fig. 1.

The loop network has an output at each time step. There are loop connections on its hidden units or point the loop connection from the output of the previous time step to the hidden unit of the current time step, and similarly, each time step corresponds to one output. The following equation gives the renewal equation related to the network forward propagation [12, 13].

$$a_t = b + Wh_{t-1} + Ux_t \tag{1}$$

$$h_t = tanh(a_t) \tag{2}$$

$$o_t = c + Vh_t \tag{3}$$

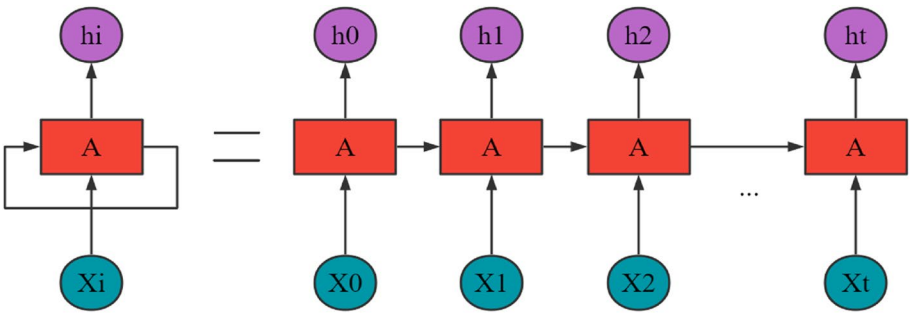

Fig. 1 Rn structure diagram

$$\widehat{y}_t = softmax(o_t) \tag{4}$$

The weight matrix U, W and the offset vector b correspond to the connection input to the hidden unit, while the weight matrix V and the offset vector c correspond to the connection from this time step to the next time step on the hidden unit.

The hidden unit h in the graph is used as the intermediate quantity between the past and the future to decouple the relationship between the past and the future so that the variable with long-distance interval can indirectly act on the output of the network through its influence h.

RNN is different from other network structures in that it can properly process data with sequence characteristics, such as a paragraph, a video, or some continuous pictures [14]. Therefore, every time a new picture is read, the network will recognize the feature information that is different from that read in the past.

At this time, the network will actively learn new features and update its own state value with the new feature information. In other words, the network will automatically use the new features to constantly improve the impression of objects in the picture in its mind and finally output a conclusion to the decoding module.

3D point cloud reconstruction of ceramic products

After being separated from the ceramic works of art and users, strictly speaking, it is a complete subversion of ancient ceramics. It integrates design and re-creation into the material carrier of ceramics, which gives the porcelain a new definition and connotation. Its uniqueness determines that people cannot live without ceramics at any time. Without ceramics, we must lack an important spiritual feeling in our life. In new works of art, ceramics and other materials are mixed together to form a new artistic expression. It brings people's hearts and the world the cultural connotation of ceramics and gives ceramic art different ideas from traditional ceramics regarding artistry and application functions.

Now, with the development of science and technology. All the new ceramics have high hardness. Traditional vases and porcelain bowls are all made by drawing blanks. Stack the selected porcelain clay into a column which is convenient for storage and use. The columnar porcelain clay is put into a porcelain turntable for professional processing. When the turntable machine is energized, it can rotate at different speeds, and the

porcelain clay is pulled into the required porcelain blank shape by hand. Through the detailed research and analysis of ceramic characteristics, through the actual investigation, as well as the production of renderings and physical objects, it is concluded that different materials can also refer to this design essentials to produce physical objects.

The input data of 3D reconstruction is a collection of images collected by cameras in different positions with unknown postures. The shooting process maps the three-dimensional points of space onto the two-dimensional image plane. The reconstruction process can be regarded as the inverse process of the shooting process. By calculating the pose of the camera, the plane points of the 2D image are back-projected into the 3D space.

Sparse point cloud reconstruction needs to restore the camera's position and attitude when shooting, which includes not only the internal orientation elements, such as the focal length, pixels, and distortion of the camera itself, but also the external orientation elements, such as rotation and translation between camera coordinate systems. In the optimization process, the re-projection error of three-dimensional points is taken as the objective function so that the external orientation elements of the camera and the coordinates of three-dimensional points can be optimized at the same time.

In the 3D point cloud reconstruction of ceramic products, the estimation of camera position and pose is a crucial step. This includes determining the internal parameters of the camera (such as focal length and pixel size) and external parameters (such as the camera's position and posture). By optimizing algorithms, the re-projection error of 3D points can be minimized, resulting in more accurate camera parameters and 3D point coordinates. In addition to estimating camera parameters, feature point extraction and matching are also important factors affecting the quality of 3D point cloud reconstruction. On the surface of ceramic products, there are often various complex textures and patterns that can be extracted and matched as feature points. By selecting appropriate feature extraction algorithms and matching strategies, the accuracy and efficiency of 3D point cloud reconstruction can be improved. The camera model is a core tool in computer vision and robot vision, used to describe how points in the 3D world are mapped onto a 2D image plane. This process involves several key coordinate systems and transformations, including the world coordinate system, camera coordinate system, image coordinate system, and pixel coordinate system. By using homogeneous coordinates, we can conveniently represent these transformations in matrix form, thereby simplifying the calculation process.

$$u \cong \begin{bmatrix} f/dx & s & x_0 \\ & f/dy & y_0 \\ & & 1 \end{bmatrix} \begin{bmatrix} R_{3\times3} & T_{3\times1} \end{bmatrix} X_W = K \begin{bmatrix} R & T \end{bmatrix} X_W = P X_W \tag{5}$$

The projection matrix P is a matrix that maps the three-dimensional world coordinate X_W to the two-dimensional image coordinate u. Usually, it can be represented as the product of the camera's internal parameter matrix K and the external parameter matrix (rotation matrix R and translation matrix t). The internal parameter matrix K of the camera is indeed only related to its internal structure, such as focal length, principal point coordinates, and potential distortion parameters (although you mentioned that distortion parameters are not related to the reconstruction process, in practical applications,

they are necessary for accurate 3D reconstruction). Through camera calibration, we can determine these parameters.

Sparse point cloud reconstruction adopts an incremental algorithm, starting from two view units and restoring the projection matrix and three-dimensional point cloud of two views [15, 16]. After that, a single new view is continuously added, while the projection beams of each camera meet the spatial point. Its objective function is the sum of the squares of the re-projection errors of all points with the same name:

$$min\sum_{i,j} d\left(\widehat{P}^i\widehat{X}_j, x_j^i\right)^2 \tag{6}$$

The formula shows that the sum of squares of the distances between the estimated re-projection point $\widehat{P}^i\widehat{X}_j$ and the actual projection point x_j^i is the smallest.

In order to segment three-dimensional ceramic products hierarchically, this chapter organizes three-dimensional ceramic products in the form of multi-tree and designs the segmentation process based on RNN, as shown in Fig. 2. The root node represents the input point cloud model information of three-dimensional ceramic products. As shown in the figure, the root node is divided into three sub-scenes: part 1, part 2, and part 3.

Next, for each part's point cloud, we use the same encoding and decoding method as the root node to recursively segment the sub-scenes.

Because the structure and working principle of the 3D laser scanning system are different, the arrangement of point cloud data obtained by scanning will be different. According to the arrangement, point cloud data can be classified into four categories [17]. Each subregion has the same characteristics. This can also be seen as classifying the point cloud data and dividing the data points with similar properties in the whole point cloud data into one class. In theory, the point cloud segmentation algorithm based on the clustering method can effectively segment the point cloud data of ceramic products. Hence, this study adopts the K-means clustering algorithm, which is the most widely used among clustering algorithms, to segment the point cloud data.

Which belongs to unsupervised learning mode. The algorithm uses Euclidean distance as a similarity measure to classify data. Until the clustering center does not change or the criterion function converges to a certain interval, the iteration ends,

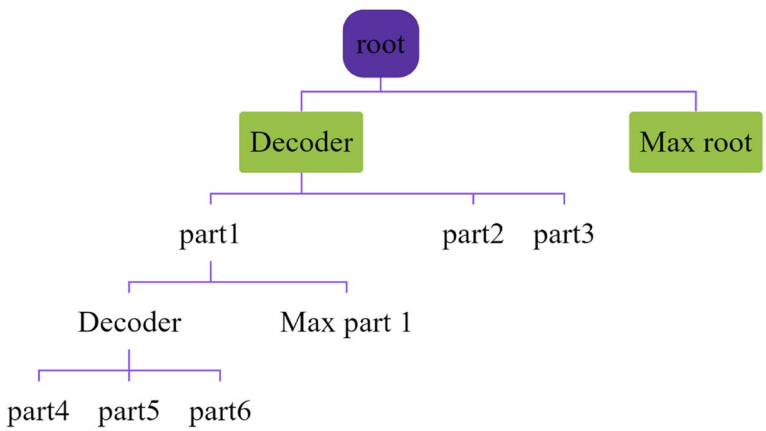

Fig. 2 Dividing the whole process of hierarchical ceramic products

and the clustering result is output. Otherwise, the iteration will continue. The formula for calculating the sum of squares is as follows:

$$SSE = \sum_{i=1}^{k} \sum_{M \in C_i} |M - b_i|^2 \tag{7}$$

where C_i is the i th cluster category, M is the sample data point in C_i, and b_i represents the cluster center of C_i.

The rotation invariance of feature points is solved by the method of gray centroid. The centroid refers to the center of the image block's gray value. This method calculates the centroid through moments and then determines the direction of the feature point by using a vector from the coordinates of the feature point to the centroid. Define its moment in the image block, as shown in Formula (8):

$$m_{pq} = \sum_{x,y \in r} x^p y^p I(x, y) \tag{8}$$

In which $p, q = \{0,1\}$ and $I\{x, y\}$ is the gray value at point (x, y).

Design semantics regards design as a language and an information symbol, expresses the language information we want to convey in the language of design, uses its own language system, accurately expresses the intention and meaning of design, and directly communicates the intercommunication between designers and audiences [18, 19].

Select random K data points as the initial clustering center and then assign each data point to the nearest category, that is, find the minimum value of Formula (9):

$$J(m, b) = \sum_{i=1}^{K} \sum_{m_j \in C_K} d(m_j, b_K) \tag{9}$$

where C_K is the set of samples in the K th category, b_K is the cluster center of all samples m_j in C_K, and $d(m_j, b_K)$ represents the Euclidean distance between sample data m_j and cluster center b_K.

In the weighted optimization matching algorithm of feature points, the outlier rate is an important parameter reflecting the matching effect and time consumption of two views. In this study, a method of sequence growth was designed. Expand the image sequence based on two views, and expand the image from the edge of the sequence every time. Assuming that the initial two views are numbered i, j, the flow of the multi-view sequence growth algorithm is shown in the following Fig. 3:

The detailed algorithm steps are as follows:

(1) Select a group of views with a lower outlier rate and absolute value less than 0.5 and add i_1, j_1 to the initial two-view sequence to complete the first sequence growth.
(2) Update the image growth edge $j_0 = j_1$ and then select the image growth from the best initial matching.
(3) Expand the multi-view sequence in the same way as in step 2.
(4) After that, manually select the views with high similarity between the two sequences and merge them if they pass the external point rate verification. Merge the series until only a few views remain.

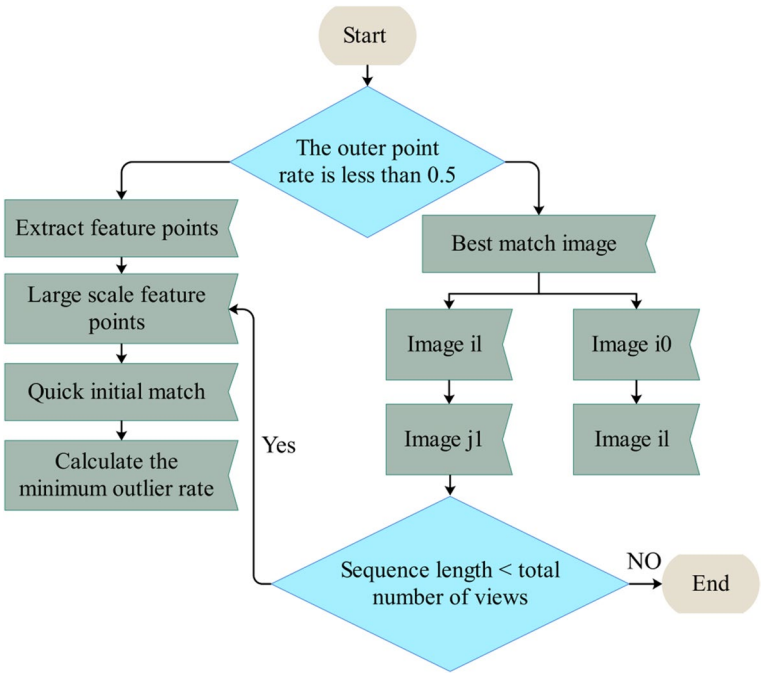

Fig. 3 Multi-view sequence growth algorithm flow

Optimization of a three-dimensional artistic design model of ceramic products

Among the three-dimensional digital technologies, 3D printing technology has become the focus of designers from all sides, and some people worldwide have begun to use it to make craft products. 3D printing technology combines the functions of three-dimensional digital design and craft manufacturing. For ceramic products, the current 3D technology can already realize dewaxing and casting glass. Therefore, when using 3D digital technology to design glass products, glass products can be finished by 3D printing technology. The model of Hunan embroidery created by the three-dimensional digital technology is very similar to the final artistic products produced by people. If you want to observe the production effect of Hunan embroidery products in advance, you can preview it by designing the model.

In addition to following the original modeling mode, ceramic modeling has its own personality. In modeling design, besides designing the modeling form of works, it also has its own independent aesthetic value. It can not only meet the needs of utility function but also give people different degrees of emotional pleasure and spiritual enjoyment psychologically. Besides psychological effects, it also has high-level aesthetic attributes. It shows that people can eliminate the constraints of the limited and external complex material world and abstract and refine the general essence from it. In the later cultural accumulation, the connotation of these forms has been continuously expanded, the implication is richer, and the aesthetics are stronger, completely eliminating the initial utilitarian trace. Nowadays, many organic forms directly learn from the research results of bionics and create new channels for dialogue and communication between man and nature.

Due to the characteristics of ceramic materials, it is different from precious metals such as gold and silver, which symbolize the status of dignitaries. It has more modern

elements and a sense of intimacy and life. Therefore, modern product design has a certain influence on the consumer groups of ceramic jewelry. From the design of ceramic ornaments in ancient China to the present, it can be seen that artisans have extracted and transformed traditional Chinese decorative patterns to give them new meanings. In ceramic jewelry, there are regular planes, free-form surfaces, spherical surfaces, etc. There are many ways to produce the surface in making jewelry, such as rolling out a large-area plane with a roller, cutting out a small-area plane with a tool knife, and manually shaping various free-form surfaces. Different faces will give people different feelings.

When the 3D laser scanner scans the object to be measured, it will get a lot of point cloud data, which will take up a lot of space in storage, operation, display, and processing, waste a lot of time, and greatly reduce the running efficiency. The surface of ceramic products is not smooth. It has texture or defect characteristics, so we need to keep enough information on the surface characteristics of ceramic products while streamlining the point cloud data of ceramic products. The high chord offset algorithm is different from the uniform sampling method to simplify the point cloud data, which overcomes the shortcomings of low simplification efficiency and ignores the curvature change of the point cloud.

Reading data one by one according to the order of scanning data by a three-dimensional laser scanner and setting a chord height threshold η_h according to Formula (10) are as follows:

$$\eta_h = \sum_{i=1}^{n} \frac{h_i}{n} \tag{10}$$

YOLOv3, as an efficient real-time object detection algorithm, provides strong support for 3D point cloud reconstruction of ceramic products with its ability in image feature extraction and encoding. When applying YOLOv3 to 3D point cloud reconstruction of ceramic products, its encoder section is responsible for extracting and encoding features of ceramic products from 2D images. These features include key information such as shape, texture, and color, which are crucial for subsequent 3D reconstruction. On the basis of maintaining the original advantages of YOLOv3, we can further enhance its feature extraction ability and make the network easier to train by improving and optimizing its model structure and algorithm. These improvements may include adjusting the number of convolutional layers, changing the configuration of residual connections, and introducing new regularization methods. When YOLOv3 is used to restore 3D objects, the first structure module, encoder, uses the structure of CNN to extract and encode the features of images, which includes 12 convolution layers and five residual connections. In this paper, while keeping the original advantages of YOLOv3 as much as possible, the structure and algorithm of its model are improved and optimized, which makes network training more difficult without deepening the depth of the network. At the same time, it strengthens the ability of the encoder to extract features and also makes the whole network easier to train. Figure 4 shows the structure of the encoder part of the improved YOLOv3.

Compared with the original network, the biggest difference of the improved YOLOv3 network lies in the addition of two dense links, which provide the network

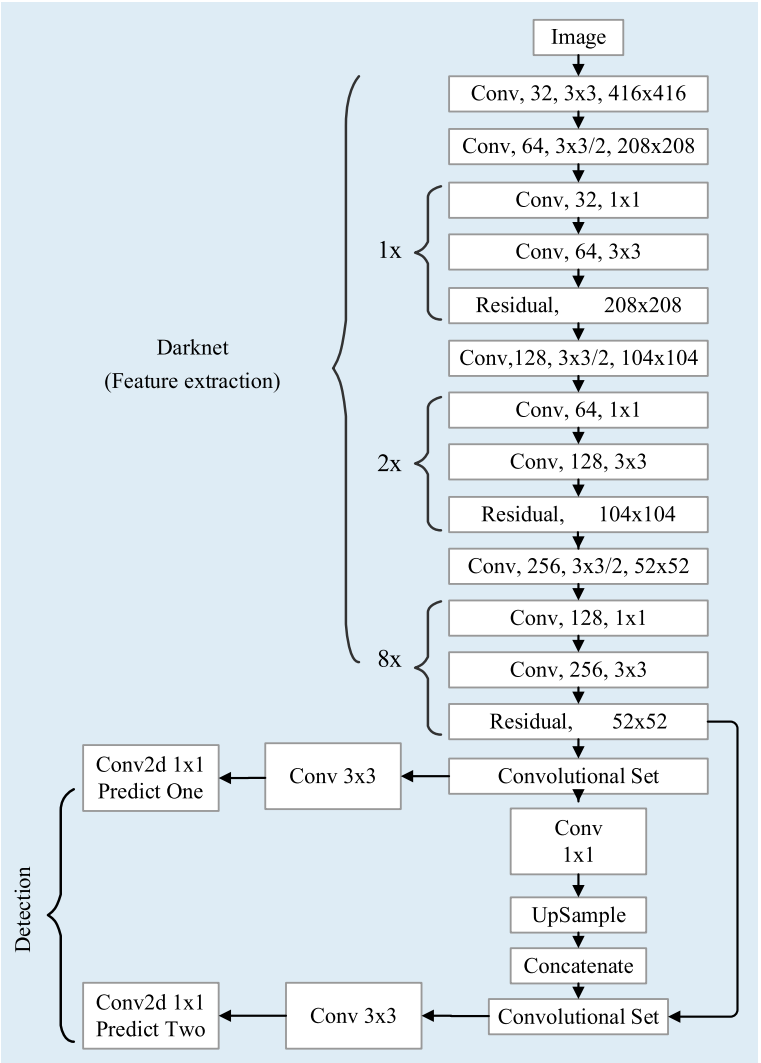

Fig. 4 Improved encoder module of post-YOLOv3

with excellent feature extraction ability so that the network can obtain more and better feature information when performing tasks [20].

$$x_l = H_l\{[x_0, x_1, \cdots, x_{l-1}]\} \tag{11}$$

The tanh function is a hyperbolic tangent function with a range of $(-1, 1)$. Its unsaturated region usually refers to the part where the function value is close to 0 but not completely equal to 0. Because within this region, the gradient of the function is relatively large, which is beneficial for updating weights during the training process.

By storing a portion of the values in the unsaturated region of the tanh function in a lookup table, we can quickly obtain these values without the need for real-time computation. When the input value to be queried is not in the table, interpolation or other methods can be used to approximate the function value. This method can improve computational speed while maintaining computational accuracy.

$$\sigma(x) = tanh\left(\frac{x}{2}\right) + \frac{1}{2} \tag{12}$$

$$tanh(x) = 2\sigma(2x) - 1 \tag{13}$$

Besides the nonlinear activation function, other key operations in the RNN network include matrix–vector multiplication and vector dot multiplication.

Fusion of multi-dimensional information, screening of useful information, and filtering of useless information to strengthen the connection between entity words and entity relations and achieve the effect of obtaining entity relations. For t each time step, the selection gate mechanism uses S, h_n, e_1, e_2 to generate the representation $h_t\prime$ of each selection gate, and its calculation formula is as follows.

$$S = \begin{bmatrix} \overrightarrow{h}_n \\ \overleftarrow{h}_1 \end{bmatrix} \tag{14}$$

$$SGate_t = \sigma(W_s h_t + U_s S + V_s e_1 + V_s e_2 + b) \tag{15}$$

$$h_t\prime = h_t \otimes SGate \tag{16}$$

where W_s, U_s, V_s is the weight vector, b is the offset value, σ represents the sigmoid activation function, and $\otimes$ represents array dot multiplication. Finally, a new sentence is obtained to represent the sequence $\{h_1\prime, h_2\prime, \cdots, h_n\prime\}$.

Results and discussion

The feature matching between two views has the constraint of epipolar geometry relation, and the coordinate relation can be established by the basic matrix to assist feature matching. In applications such as stereo vision, motion recovery structures (SFM), or visual odometry, it is usually necessary to find corresponding points from two or more views to estimate the relative pose or basic matrix between cameras. However, due to factors such as noise, occlusion, and changes in lighting, the original feature matching results often contain errors and mismatches. Transforming the problem into finding the optimal matching pair from the original matching results containing errors and mismatches is a typical optimization problem. The commonly used method includes the RANSAC (random sampling consistency) algorithm, which iteratively randomly extracts the minimum sample set (usually 8-point pairs for basic matrix estimation) from the original matching. Then verify whether these points satisfy a certain geometric constraint (such as epipolar constraint) to find the optimal matching pair.

In order to verify the rationality of the weighting algorithm, 2 ceramic images were selected in this study, and 3638 pairs of feature points were obtained by initial matching, which were arranged in the order of scale from largest to smallest, as shown in Fig. 5.

When it is mentioned that the fluctuation of the average distance between each group increases with the increase of feature point scale, this usually means that it is on larger-scale feature points. Due to differences in image resolution or local texture, the matching distance of feature points between different groups varies more. This

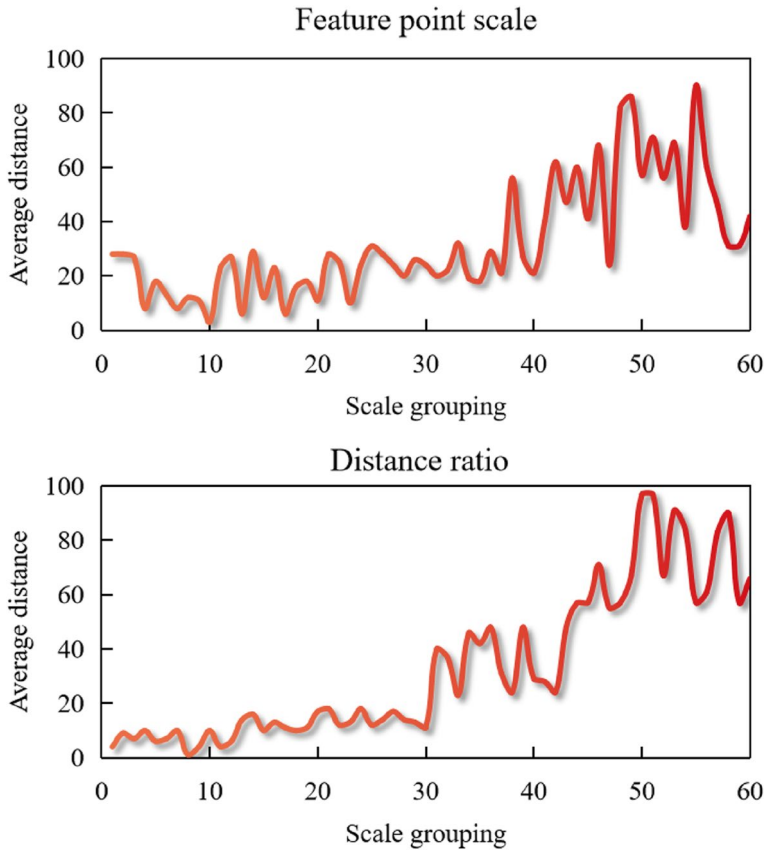

Fig. 5 Relationship between epipolar geometry error and characteristic point scale and distance ratio

Table 1 Each view reprojects RMSE

View number	RMSE	View number	RMSE
1	0.4042	6	0.6221
2	0.4108	7	0.5487
3	0.4303	8	0.657
4	0.4222	9	0.5203
5	0.4245	10	0.5837

fluctuation may be influenced by various factors, such as image noise, lighting conditions, and scale changes.

To reduce this fluctuation, a multi-scale feature extraction method can be considered to capture feature points of different scales. In addition, utilizing robust feature matching algorithms such as RANSAC and MSAC can also help reduce mismatches and reduce fluctuations in average distance. The error level of the analysis result, RMSE (root-mean-square error) of each view, is shown in the following Table 1.

As shown in Table 1, the re-projection RMSE of 10 views is less than 1 pixel.

In this chapter, the public data set is used for the experiment. Figure 6 shows the training accuracy and loss function curve of the point cloud deep learning network

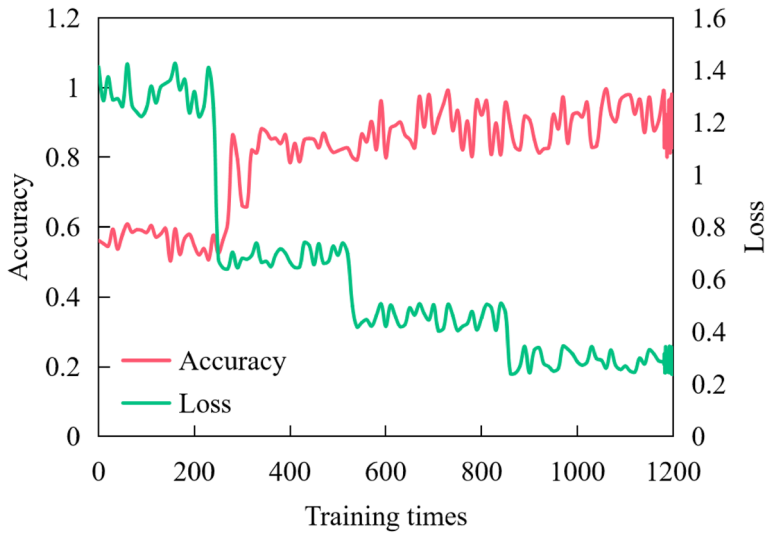

Fig. 6 Accuracy of network training and curve of the loss function

Table 2 Segmentation result

Method	Accuracy	Recall	F1
Literature [4]	77.36	71.25	69.82
Literature [5]	81.21	76.39	72.18
Methods of this paper	91.25	88.36	80.27

in segmentation tasks. These curves are important indicators for evaluating the performance of deep learning models. The accuracy curve reflects the predictive ability of the model to test data during the training process, while the loss function curve reflects the error changes of the model during the training process. By analyzing these curves, we can understand the training effectiveness of the model and adjust its parameters or structure accordingly to optimize its performance.

As the training progresses, the accuracy of the network gradually improves, reflecting the gradual optimization of the network during the learning process. When the accuracy stabilizes at 95%, it indicates that the network is able to accurately recognize and process objects in most scenarios. This stability is crucial for practical applications as it ensures that the network can maintain high performance even when facing new data.

As shown in Table 2, these are partial segmentation results of three networks on the data set.

According to Table 2, compared with references [4] and [5], the accuracy of this method in ceramic segmentation is improved. No matter in the same scene or different scenes, the same kind of objects can be accurately segmented, and there are obvious differences between different objects. Therefore, this method network has good performance in segmentation tasks.

In numerical calculations, the choice of numerical format directly determines the range and accuracy of data representation. For RNN networks, internal parameter

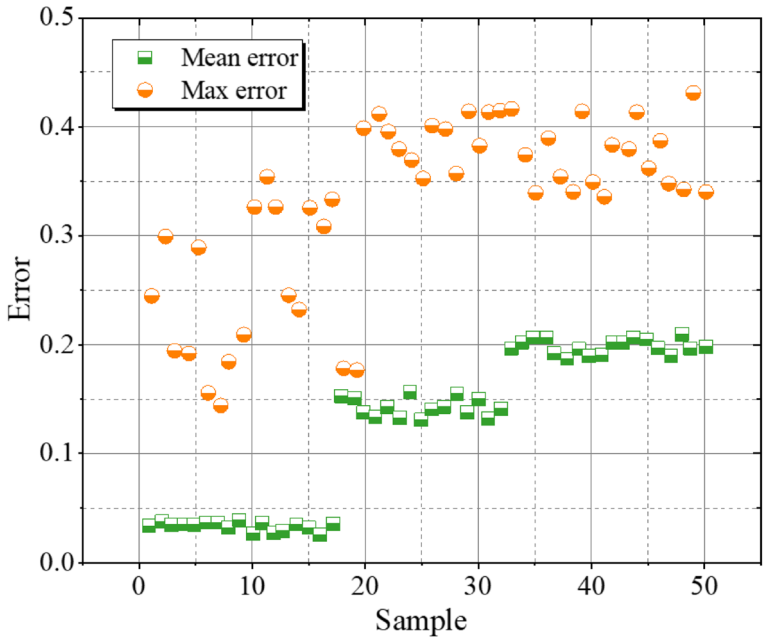

Fig. 7 Network calculation errors under different numerical schemes

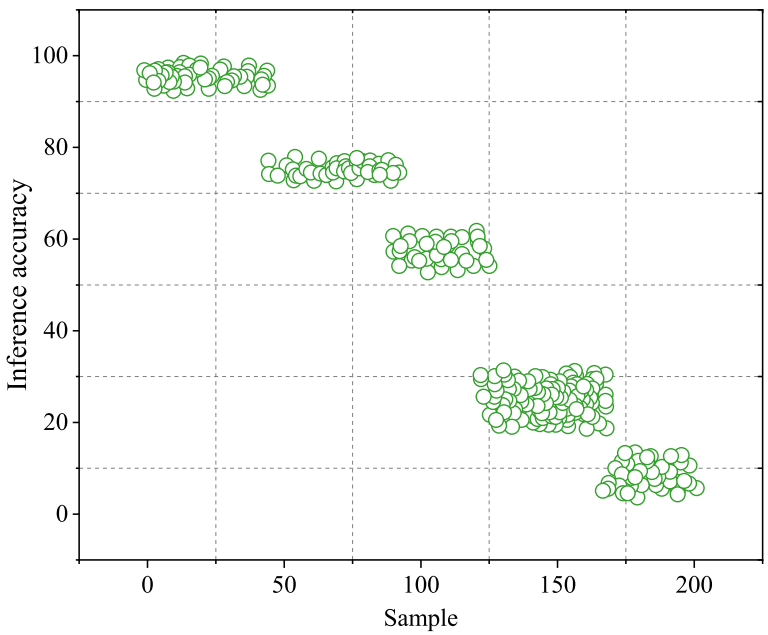

Fig. 8 Inference accuracy in different numerical formats

updates and calculations rely on precise numerical representations. We tested various numerical formats including fixed point, floating point, and mixed precision.

Figures 7 and 8 show the inference accuracy curves of RNN networks under different numerical formats. From the figure, it can be seen that the floating-point format maintains high accuracy in the inference process due to its high-precision characteristics. However, although the fixed-point format is more resource efficient, it may lead to

a decrease in accuracy when dealing with complex tasks due to accuracy loss. The mixed precision format combines the advantages of floating-point and fixed-point numbers to maintain a certain level of accuracy while reducing resource consumption.

The numerical format and optimization methods used in this design pay special attention to ensuring accuracy while minimizing the use of hardware resources. Compared with traditional implementations that use high precision and large dynamic ranges, this design not only reduces hardware resource consumption and costs but also achieves a reasonable balance between performance and resources. This compromise solution enables RNN accelerators to maintain high inference accuracy while also having a higher-energy efficiency ratio, making them suitable for various resource-constrained application scenarios.

In addition, in this section, we also verified the performance of the improved YOLOv3 network in terms of training speed. YOLOv3 is an advanced real-time object detection algorithm with excellent speed and accuracy performance. To evaluate the effectiveness of the improved network, we selected 5 randomly selected datasets from the database, containing a total of 4055 objects. By comparing the training speed before and after improvement, we found that the improved YOLOv3 network had a significant improvement in training speed.

Compared with traditional convolutional networks, regulatory information in dense link networks no longer relies solely on the output of the previous layer. In traditional convolutional networks, due to the information being transmitted layer by layer, as the network depth increases, it is difficult for lower layers to receive regulatory information from higher layers, which often leads to gradient vanishing problems and makes training difficult. However, in DenseNet, since each layer is connected to all previous layers, regulatory information can be directly backpropagated from the loss function to each layer of the network, achieving more effective regulation Table 3.

The advantage of this deep regulation is that it helps the network better learn the feature representation of data. Due to the fact that each layer can directly receive gradient information of the loss function, the network can better adjust its parameters to meet task requirements. In addition, since each layer in the network can directly access the original input information, this also helps the network better retain useful information in the original data, thereby improving the performance of the model.

The following paper will continue to test on the testing machine, this time comparing the model coincidence rate of each method for each kind of object, and the results are shown in Fig. 9.

It can be seen that the improved New YOLOv3 is superior to the original network in almost every kind of reconfiguration. If all things are considered, the reconstruction effect of the model proposed in this paper is not as good as that of reference [4] to

Table 3 Training speed comparison

Method	Time (min)
Literature [4]	7.31
Literature [5]	6.68
Methods of this paper	3.94

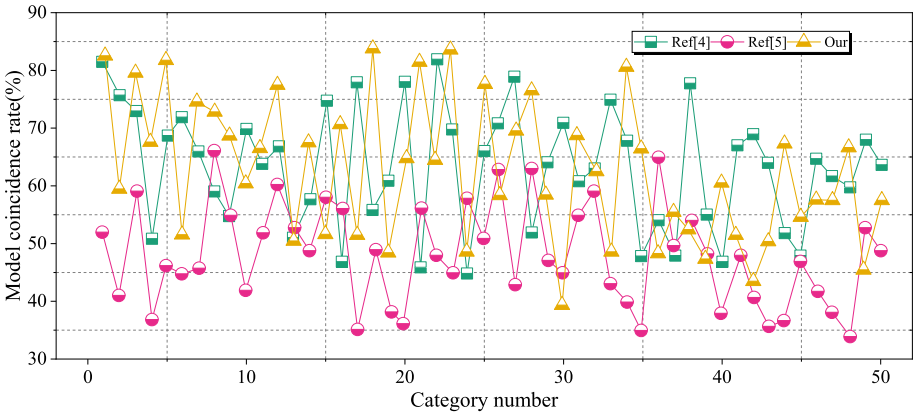

Fig. 9 Coincidence rate of the prediction model and real model

some extent, but the time efficiency is faster than that of reference [4] by more than 50%. Therefore, on the whole, the model proposed in this paper is better than that in reference [4].

Conclusions

The "language" of ceramics refers to the visual expression formed by its unique elements such as shape, color, and texture. These elements are achieved in traditional craftsmanship through the hands of craftsmen and years of accumulated experience. However, the application of three-dimensional digital technology makes the creation and expression of these elements more efficient and precise. A new 3D YOLOv3 framework is proposed, which makes RNN change from only being able to memorize 2D knowledge to 3D information. It takes it as the core of the whole network to realize the task of 3D reconstruction of a single image or multiple images. After training for a certain number of times, the network gradually becomes stable, the accuracy rate is kept at 95%, and the loss function value is reduced below 0.2. It realizes the finer segmentation of the three-dimensional scene and clearer understanding and cognition. The communication between man and machine can bring us beautiful visual enjoyment, provide more imagination space for our design, and reflect that the development of modern science and technology is constantly changing our living environment and shortening the gap between ideal and reality.

Abbreviations

RNN	Recurrent neural network
3D YOLOv3	Three-dimensional You Only Look Once version 3
CNN	Convolutional neural network

Symbols

at	Activation at time t
ht	Hidden state at time t
ot	Output at time t
yt	Predicted output at time t
b	Bias term in neural networks
W	Weight matrix in neural networks
U	Weight matrix between input and hidden layers
V	Weight matrix between hidden and output layers
x_t	Input at time t

Greek symbols

σ	Sigmoid activation function
tanh	Hyperbolic tangent activation function

Authors' contributions

JS, writing—original draft preparation, conceptualization, supervision, and project administration. XW, language review, methodology, and software.

Funding

Not applicable.

Availability of data and materials

The datasets used and analyzed during the current study are available from the corresponding author on reasonable request.

Declarations

Competing interests

The authors declare that they have no competing interests.

Received: 1 May 2024 Accepted: 14 June 2024
Published online: 09 July 2024

References

1. Jiang L, Wu X-J, Kittler J (2019) Pose-invariant three-dimensional face reconstruction. J Electron Imaging 28:53003
2. Neusser TP, Hanke F, Haszprunar G, Jörger KM (2019) 'Dorsal vessels'? 3D-reconstruction and ultrastructure of the renopericardial system of Elysia viridi s (Montagu, 1804)(Gastropoda: Sacoglossa), with a discussion of function and homology. Journal of Molluscan Studies 85:79–91
3. Chen Zhangwei, Li Ziyong, Li Junjie, Liu Chengbo, Lao Changshi, Yuelong Fu, Liu Changyong, Li Yang, Wang Pei, He Yi (2019) 3D printing of ceramics: a review. Journal of the European Ceramic Society. 39(4):661–687 (ISSN 0955–2219)
4. Chen Z, Sun X, Shang Y, Xiong K, Xu Z, Guo R, Zheng C (2021) Dense ceramics with complex shape fabricated by 3D printing: a review. Journal of Advanced Ceramics 10:195–218
5. Dal PAMDO, Bottino MA, Anami LC, Werner A, Kleverlaan CJ, Lo GR, Tribst JPM (2021) Toothbrushing wear resistance of stained CAD/CAM ceramics. Coatings. 11(2):224
6. Doodi R, Gunji B-M (2023) Prediction and experimental validation approach to improve performance of novel hybrid bio-inspired 3D printed lattice structures using artificial neural networks. Sci Rep 13(1):7763
7. Fang Z, Wang R, Wang M, Zhong S, Ding L, Chen S (1963) Effect of reconstruction algorithm on the identification of 3D printing polymers based on hyperspectral CT technology combined with artificial neural network. Materials 13(8):20202
8. Hu F, Mikolajczyk T, Pimenov D-Y, Gupta M-K (2021) Extrusion-based 3D printing of ceramic pastes: mathematical modeling and in situ shaping retention approach. Materials 14(5):1137
9. Xu S, Xia M, Gu R, Yin Y, Xu L, Xia Y, Yin J (2019) Three-dimensional modeling of magneto-optical trapping of MgF molecules with multilevel rate equations. Phys Rev A (Coll Park) 99:033408
10. Bueno J, Maktoobi S, Froehly L, Fischer I, Jacquot M, Larger L, Brunner D (2018) Reinforcement learning in a large-scale photonic recurrent neural network. Optica 5:756–760
11. Ndikumana E, Ho Tong Minh D, Baghdadi N, Courault D, Hossard L (2018) Deep recurrent neural network for agricultural classification using multitemporal SAR Sentinel-1 for Camargue. France Remote Sens (Basel) 10:1217
12. Whangbo T-K, Eun S-J, Jung E-Y, Park DK, Kim SJ, Kim CH, Chung KJ, Kim K-H (2018) Personalized urination activity recognition based on a recurrent neural network using smart band. Int Neurourol J 22:S91
13. Cheng L, Zang H, Ding T, Sun R, Wang M, Wei Z, Sun G (2018) Ensemble recurrent neural network based probabilistic wind speed forecasting approach Energies (Basel) 11:1958
14. Zhang W, Du Y, Yoshida T, Wang Q (2018) DRI-RCNN: an approach to deceptive review identification using recurrent convolutional neural network. Inf Process Manag 54:576–92
15. Ganjefar S, Tofighi M (2018) Optimization of quantum-inspired neural network using memetic algorithm for function approximation and chaotic time series prediction. Neurocomputing 291:175–186
16. Qiu Q (2022) The application of neural network algorithm and embedded system in computer distance teach system. J Intell Syst 31:148–158
17. Yu Y, Chen Y, Li Y, Gao Z, Gai Z, Zhou Y (2022) SQNN: a spike-wave index quantification neural network with a pre-labeling algorithm for epileptiform activity identification and quantification in children. J Neural Eng. 19:016040
18. Jin WU, Qianwen SHI, Meng XI, Lei W, Huadie Z (2022) An improved micro-expression recognition algorithm of 3D convolutional neural network. High Technology Letters 28:63–71
19. Farfan CA, Epstein J, Turner DB (2018) Femtosecond pulse compression using a neural-network algorithm. Opt Lett 43:5166–5169
20. Wang W, Tang R, Li C, Liu P, Luo L (2018) A BP neural network model optimized by mind evolutionary algorithm for predicting the ocean wave heights Ocean Engineering 162:98–107

Publisher's Note